Radiation Physics and Chemistry ∎ (∎∎∎∎) ∎∎∎–∎∎∎

Contents lists available at ScienceDirect

Radiation Physics and Chemistry

journal homepage: www.elsevier.com/locate/radphyschem

Radiation damage within nucleoprotein complexes studied by macromolecular X-ray crystallography

Charles S. Bury [a], Ian Carmichael [b], John E. McGeehan [c], Elspeth F. Garman [a,*]

[a] Laboratory of Molecular Biophysics, Department of Biochemistry, University of Oxford, South Parks Road, Oxford OX1 3QU, UK
[b] Notre Dame Radiation Laboratory, University of Notre Dame, Notre Dame, IN 46556, USA
[c] Molecular Biophysics, Institute of Biomedical and Biomolecular Sciences, University of Portsmouth, King Henry 1st Street, Portsmouth PO1 2DY, UK

HIGHLIGHTS

- We review radiation damages nucleoprotein complexes during X-ray crystallography.
- We detect radiation-induced chemical changes from electron density difference maps.
- We use a systematic pipeline to track electron density loss with increasing dose.
- Nucleic acids are radiation-insensitive compared to protein within crystals at 100 K.
- RNA protects key RNA-binding residues from radiation-induced decarboxylation.

ARTICLE INFO

Article history:
Received 1 April 2016
Accepted 25 May 2016

Keywords:
Protein-nucleic acid complexes
Macromolecular X-ray crystallography
Radiation damage
Electron density
Dose

ABSTRACT

In X-ray crystallography, for the determination of the 3-D structure of macromolecules, radiation damage is still an inherent problem at modern third generation synchrotron sources, even when utilising cryo-crystallographic techniques (sample held at 100 K). At doses of just several MGy, at which a typical diffraction dataset is collected, site-specific radiation-induced chemical changes are known to manifest within protein crystals, and a wide body of literature is now devoted to understanding the mechanisms behind such damage. Far less is known regarding radiation-induced damage to crystalline nucleic acids and the wider class of nucleoprotein complexes during macromolecular X-ray crystallography (MX) data collection. As the MX structural biology community now strives to solve structures for increasingly larger and complex macromolecular assemblies, it essential to understand how such structures are affected by the X-ray radiation used to solve them. The purpose of this review is to summarise advances in the field of specific damage to nucleoprotein complexes and to present case studies of MX damage investigations on both protein-DNA (C.Esp1396I) and protein-RNA (TRAP) complexes. To motivate further investigations into MX damage mechanisms within nucleoprotein complexes, current and emerging protocols for investigating specific damage within $F_{obs}(n) - F_{obs}(1)$ electron density difference maps are discussed.

1. Introduction

Over the past century, macromolecular X-ray crystallography (MX) has proved an invaluable tool within structural biology, permitting the three-dimensional visualisation of proteins and nucleic acids at near atomic resolution. As of early 2016, a total of 104,244 structures of proteins and nucleoprotein complexes have been deposited within the Protein Data Bank (PDB); this world-wide effort has been instrumental in the correct characterisation of the molecular interactions underpinning the function of highly biologically-important macromolecules (Ferreira et al., 2004; Voorhees et al., 2009).

During a standard MX experiment, crystalline macromolecular samples are exposed to a monochromatic beam of ionising X-rays (with typical energies 8–15 keV) in order to generate a series of diffraction images, from which a temporal and spatial average of the macromolecular electron density throughout a crystal can be derived. However, for a typical 100 μm thick protein crystal exposed to a 12.4 keV X-ray beam, only a small proportion (2%) of incident photons are predicted to actually interact directly with the crystal, with only 8% of these elastically scattering to contribute to the desired diffraction pattern. The photoelectric and Compton effects are the dominant processes by which the incident

* Corresponding author.
E-mail addresses: charles.bury@dtc.ox.ac.uk (C.S. Bury), elspeth.garman@bioch.ox.ac.uk (E.F. Garman).

http://dx.doi.org/10.1016/j.radphyschem.2016.05.023

photon energy is absorbed by the crystal (84% and 8% respectively) (Garman, 2010). Consequently, for the current third generation high-brilliance synchrotron sources with photon fluxes in the range of 10^{10}–10^{13} ph/s into a 5–100 μm diameter spot, this results in a large deposition of energy within typical macromolecular crystals upon an X-ray exposure of a few frames of data collection.

The dose is defined as the energy absorbed in the crystal per unit mass (with units of gray, Gy=J/kg); protein crystals typically accumulate doses of the order of several MGy within the course of one diffraction dataset collection at 100 K. Increasing dose is coupled with increasing crystal non-isomorphism, eventually leading to *global radiation* damage effects: an overall reduction in the mean diffraction intensity, loss in resolution, and increases in both crystal mosaicity and unit cell volume (Murray and Garman, 2002; Ravelli and Garman, 2006; Weik et al., 2000). An experimental dose limit ($D_{0.7}$) of 30 MGy has been determined, cited as the upper dose at which the average diffraction intensity for *any* protein crystal held at 100 K will have decayed to 70%, and at which the biological information derived from the inferred structure of the crystalline protein may be compromised (Owen et al., 2006). Due to these various effects, radiation damage is still an inevitable hindrance to successful MX data collection and structure determination, even with the crystal held at cryocooled temperatures (100 K) and with modern advances in multi-crystal data collection methods (Stellato et al., 2014), high X-ray flux density nano- and micro-beamlines (I24) and faster pixel based detectors, also at room temperature (RT) (Owen et al., 2014). Such issues are exacerbated as experimenters push towards structure determination of larger and more complex macromolecules, which in turn typically involve collecting data from smaller crystals (< 1–5 μm). These have fewer unit cells compounded with intrinsic crystal disorder, resulting in weaker diffraction. There must always be a compromise between collecting more diffraction data and the inevitable progression of radiation damage with increasing dose.

Even before any observed reduction in diffraction resolution, at doses of several MGy, synchrotron X-ray irradiation has been widely reported to induce site-specific chemical and conformation changes to crystalline proteins held at 100 K. Such damage has been directly observable within electron density maps reconstructed from sequential diffraction patterns obtained with increasing dose (Weik et al., 2000) (Fig. 1), and a reproducible order of susceptibility has now been established within a variety of proteins at 100 K: metallocentre reduction, disulphide bond elongation and cleavage, acidic residue decarboxylation, and reported Tyr –OH group disordering and methionine S_δ–C_ε bond cleavage (Burmeister, 2000; Weik et al., 2000; Yano et al., 2005). The prevalence of these *specific radiation damage* (SRD) effects are suspected to be highly dependent on local crystalline protein environment, with factors such as solvent accessibility, proximity to high X-ray cross-section atoms, acidic residue protonation state and packing density (Fioravanti et al., 2007; Gerstel et al., 2015) predicted to affect the damage rates. However, investigations into a number of protein systems have revealed minimal correlation between such individual factors and SRD events, and it is thus suggested that a multitude of parameters contribute to a particular residue's susceptibility to SRD (Holton, 2009). For instance, the addition of a single ordered nitrate anion (NO_3^-) proximal to a disulphide bond will result in substantial stability of the otherwise highly reducible bond (De La Mora et al., 2011). At doses below 1 MGy, disulphide bond radicalisation (a precursor for disulphide breakage) has been detected by electron paramagnetic resonance (EPR) and *in situ* UV–visible absorption microspectrophotometry (Sutton et al., 2013). Radiation-induced structural changes within active sites of photosensitive proteins have also been detected at doses as low as 0.06 MGy (Borshchevskiy et al., 2014). As such, it is unclear whether a universal safe dose is achievable in MX before the onset of protein specific damage events.

Somewhat paradoxically, given the wealth of radiation damage studies on nucleic acids conducted by radiation chemists (e.g. (Alizadeh et al., 2015; Cadet et al., 1999; Michaud et al., 2012)), crystallographic investigations regarding MX radiation-induced changes to nucleic acids and the larger class of nucleoprotein complexes have been substantially less comprehensive to date, and a governing MX specific damage *rulebook* for them has not yet been established. Nucleic acid and nucleoprotein complexes now comprise approximately 6.4% of MX-derived structures deposited within the PDB. The structural biology community are currently pursuing increasingly large (> 200 kDa) and complex macromolecular systems encompassing those bound to nucleic acids, and a thorough characterisation of MX radiation damage within such complexes is essential to ensure correct structural interpretations at the atomistic scale provided by crystallography.

Nucleic acids have diverse roles in information exchange and control but also make up some of the fundamental structural and catalytic components of large macromolecular machines such as ribosomes and spliceosomes. A multitude of studies have investigated both nucleic acids and nucleoprotein complexes in solution at RT, where secondary diffusive hydroxyl radicals produced through solvent radiolysis can add to double covalent bonds within both DNA and RNA bases to induce SSBs and base modification (Chance et al., 1997; Spotheim-Maurizot and Davidkova, 2011), and oxidise protein residues with differential degrees of susceptibility (O'Neill et al., 2002). However many radical species (such as hydroxyl radicals) are immobilised below 110 K (Allan et al., 2013; Owen et al., 2012); since most modern MX experiments take place at 100 K, such hydroxyl-mediated damage is not

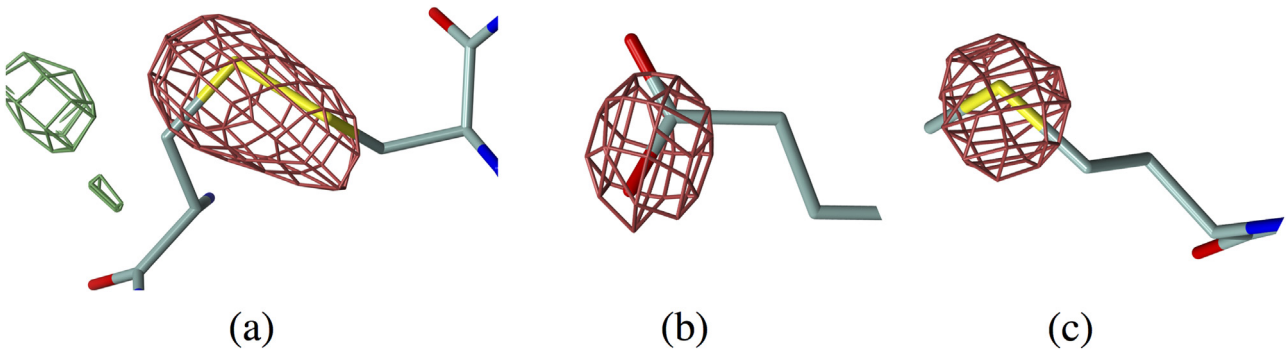

Fig. 1. (a) Disulphide bond cleavage, (b) Glu decarboxylation, and (c) Met sulphur disordering within *Torpedo californica* acetyl-cholinesterase (TcAChE) pdb: 1QID (Weik et al., 2000). $F_{obs}(5)-F_{obs}(1)$ Fourier difference maps between dataset 1 and 5 collected on the same crystal are shown, contoured at $\pm 4\sigma$, with negative difference density (red) indicating disordering of the atomic positions with accumulated dose. F_{obs} is the set of observed structure factors, proportional to the square root of the observed intensities recorded on the diffraction pattern. (For interpretation of the references to color in this figure legend, the reader is referred to the web version of this article.)

Please cite this article as: Bury, C.S., et al., Radiation damage within nucleoprotein complexes studied by macromolecular X-ray crystallography. Radiat. Phys. Chem. (2016), http://dx.doi.org/10.1016/j.radphyschem.2016.05.023

anticipated. Instead, the main damaging species are predicted to be low energy electrons (LEEs) with energies of several eV. After primary photoabsorption of an incoming X-ray photon by both the macromolecule and crystal solvent channels, each ejected high-energy primary photoelectron (as well as associated Auger electrons) is predicted to have enough energy to cause the production of up to ~500 secondary LEEs along their track length (3–4 μm for the incident energies employed in MX (Nave and Hill, 2005; Sanishvili et al., 2011)). These LEEs can then cause further ionisation events as they gradually thermalise throughout the crystal (O'Neill et al., 2002).

Electrons have been shown to be mobile at 77 K (Jones et al., 1987), with electron spin resonance (ESR) spectroscopy studies postulating rapid quantum tunnelling along both the protein backbone and nucleic acid stacked base π-systems as the dominant mechanism by which LEEs can relocate from initial ionisation sites at 100 K (Symons, 1997). Ultimately, these LEEs become trapped by electron-affinic sites in both protein and nucleic acid to form electron gain centres in proteins and $T^{\bullet-}$ and $C^{\bullet-}$ centres in nucleic acids. Positive holes are also believed to migrate at 100 K, but to a lesser extent, being more readily trapped, predominantly by deprotonation at protein backbone amide units and at acidic residue side-chain carboxyl groups, and to form $G^{\bullet+}$ centres in nucleic acids.

Extensive studies on sub-ionisation level LEEs (0–15 eV) interacting with short DNA oligonucleotides deposited on films at varying degrees of hydration at RT, 4 K, and 70 K have been performed to date (Alizadeh and Sanche, 2014; Ptasinska and Sanche, 2007). Transient resonant attachment by LEEs to π^* orbitals of DNA bases and the sugar-phosphate backbone, followed by rapid bond dissociation, is now believed sufficient for cleavage of both base-sugar N_1C bonds and strong (~4 eV) covalent bonds within the DNA phosphodiester backbone (Barrios et al., 2002; Berdys et al., 2004; Simons, 2006), with computational chemistry calculations indicating preferential cleavage of sugar-phosphate C–O bonds over other bonds present within the DNA structure (Théodore et al., 2006). Such bond ruptures are ultimately detected as yields of single strand breakages (SSBs), typically through gel electrophoresis analysis (Boudaïffa, 2000). Similar preferential rupture of C–O bonds (in particular the 5′ C–O bond) has been reported in a recent X-ray absorption spectroscopy study for DNA oligonucleotides in solution under either UVA photon or proton irradiation (Czapla-Masztafiak et al., 2016).

Such LEE-mediated damage observations are thus also anticipated within crystalline DNA at 100 K upon ionising X-ray radiation exposure. However, an MX investigation coupled with Raman spectroscopy (McGeehan et al., 2007) into X-ray radiation-induced damage to cryocooled brominated oligonucleotide crystals observed no clear signs of native DNA specific damage, with DNA debromination as the only chemical change detected, even at the highest accumulated dose tested (> 15 MGy). Although anecdotal reports suggest that native DNA is substantially resilient to X-ray irradiation at the MGy doses typically reported for MX data collection (with no clear or reproducible deterioration of the electron density with accumulated dose), this remains to be systematically tested and characterised.

The following sections provide a discussion of MX radiation damage case studies on two bacterial nucleoprotein complexes: the C.Esp1396I-DNA complex and the TRAP-RNA complex. In previous studies, MX protein specific damage has been typically characterised by visually interpreting $F_{obs}(n)-F_{obs}(1)$ Fourier difference maps. However such time consuming visual inspection is limited by the subjective bias of the investigator. The development of scripted pipelines is discussed, designed to mitigate such bias and systematically categorise radiation-induced chemistry within the current crystalline nucleoprotein case studies. Such automated approaches are applicable to any MX protein or nucleic acid crystal study, with the case studies presented here designed to motivate further MX specific damage systematic investigations.

2. The C.Esp1396I-DNA complex: a model protein-DNA MX damage investigation

To characterise and investigate the apparent DNA radiation-insensitivity that was observed for native DNA crystals at 100 K, the relative rates of specific damage have recently been determined for a well-studied bacterial protein-DNA complex (Bury et al., 2015) (C.Esp1396I, pdb: 3clc, resolution: 2.8 Å (McGeehan et al., 2008)).

'Controller' C-protein dimers, such as C.Esp1396I, are part of a large helix-turn-helix protein family, acting as transcriptional regulators of gene expression in both eukaryotic and prokaryotic systems. In the C.Esp1396I complex (Fig. 2), C-protein dimers (chains A and B, and C and D) bind to the 35bp DNA operator sequence (chains E and F) of a bacterial restriction-modification (R-M) system Esp1396I, to regulate C-protein and endonuclease gene expression in a concentration-dependent manner (Ball et al., 2009). The C.Esp1396I complex (~60 kDa) was chosen as a model biologically-relevant protein-DNA complex due to the large 35bp dsDNA component, resulting in the number of protein and DNA atoms being of the same order (protein: 2496 atoms, DNA: 1429 atoms). A statistical comparison was conducted between SRD rates to interacting DNA and protein constituents, determining protein to be significantly more damage susceptible within the complex over the wide dose range investigated (2.1–44.6 MGy over 8 MX datasets, n = 1,..,8, collected on the same crystal held at 100 K) (Bury et al., 2015).

As is conventionally performed in protein MX specific damage studies (Southworth-Davies et al., 2007), sites of significant radiation-induced electron density disordering within the C.Esp1396I complex were located by calculating Fourier difference maps with increasing dose ($F_{obs}(n)-F_{obs}(1)$ for n = 2, …, 8) over the crystal asymmetric unit. Difference peaks within $F_{obs}(n)-F_{obs}(1)$ maps provide a visual representation of regions of high electron density loss or gain with accumulated crystal dose. For the C.Esp1396I complex, within the first difference map ($F_{obs}(2)-F_{obs}(1)$, 6.2 MGy) clear density loss was localised around acidic residue side-chain carboxyl groups, indicative of radiation-induced decarboxylation, and around methylthio sidechain groups, consistent with Met CH_3–S covalent bond cleavage (Fig. 2(a)-(b)). Such observations were highly consistent with previous reports of protein SRD (Weik et al., 2000) (no disulphide bonds are present within this protein).

At higher doses (> 14.4 MGy), several locations of SRD were detected in close proximity (within 2 Å) of the DNA, including possible sugar-phosphate C–O bond cleavage between the T24 and A25 nucleotides of DNA chain F (Fig. 2(c)–(d)). Additionally, positive electron density accumulation was observed with increasing dose near the T24 and A25 bases; this is consistent with mechanisms of LEE attachment to nucleobases as suggested within oligonucleotide film studies (Alizadeh et al., 2013), or base modification induced by close proximity solvent free radicals (Cadet et al., 1999) (for example, hydroxyl radical binding to carbon 6 in T24). The location of such a SSB correlates with a DNA region that is both AT-rich and under significant strain as a consequence of large-scale deformation due to protein binding. Our suggestion is that such strained geometries could enhance radiation damage effects in DNA and would have major biological consequences, since eukaryotic DNA wrapping around histones in part relies on the distortion of DNA around such AT-rich sites.

Whereas $F_{obs}(n)-F_{obs}(1)$ Fourier electron density difference

Please cite this article as: Bury, C.S., et al., Radiation damage within nucleoprotein complexes studied by macromolecular X-ray crystallography. Radiat. Phys. Chem. (2016), http://dx.doi.org/10.1016/j.radphyschem.2016.05.023

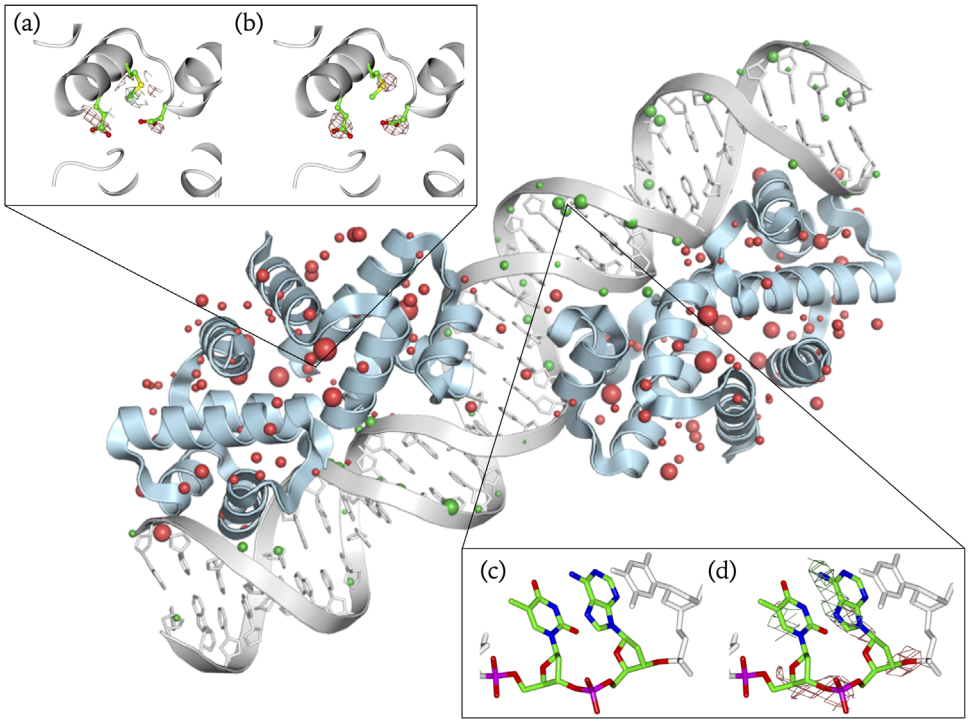

Fig. 2. (centre) The C.Esp1396I complex crystal asymmetric unit. Two C-protein dimers (chains A and B, left, and chains C and D, right) bind to the 35bp DNA operator sequence (chains E and F). Spheres represent sites of detected SRD within the highest dose dataset (44.6 MGy); red/green spheres indicate protein/DNA damage, with the sphere radii representing the magnitude of electron density loss at each SRD site. (inserts) Protein and DNA damage sites in C.Esp1396I: (a)–(b) protein chain D, Glu-54, Met-57 and Asp-64 (green, left to right), and (c)–(d) DNA chain F nucleotides T24 and A25 (with 5′ to 3′ end from left to right in each image) at (a), (c) low-dose (6.2 MGy) and (b), (d) high dose (44.6 MGy). $F_{obs}(n)-F_{obs}(1)$ Fourier difference maps are contoured at $\pm 3.0\sigma$ in green/red throughout. (For interpretation of the references to color in this figure legend, the reader is referred to the web version of this article.)

map peaks coincident with the C.Esp1396I complex provide an insight into SRD events, with increasing dose, difference maps become intrinsically noisy due to overall degradation of diffraction data quality (global radiation damage) and increasingly unmodelled chemistry within crystal bulk solvent regions. Accordingly, for the C.Esp1396I complex at 44.6 MGy, 10^3 difference peaks were detected above a 0.04 $eÅ^{-3}$ threshold (at which damage sites had been visually distinguishable from noise within the lowest dose $F_{obs}(2)-F_{obs}(1)$ difference map). To facilitate case-by-case inspection of difference peaks, a custom *python*-scripted pipeline (Bury et al., 2015) was implemented to systematically and objectively isolate damage sites throughout the C.Esp1396I complex with increasing dose (Fig. 3). Using this protocol, significant damage was detected for Asp, Glu, Met and Ser residues (electron density loss indicating disordering of the Ser side-chain –OH) even at the lowest doses (Fig. 3(a)). At higher doses, Arg and Asn exhibit electron density loss/disorder to their main-chain carboxyl group oxygen, and Ile and Lys experience partial density loss around the side-chain aliphatic and lysyl side-chains respectively. The remaining amino acids exhibited minimal SRD even at very high dose. Overall the detected damage onset was at significantly higher doses for DNA than for protein component (>20.6 MGy versus >6.2 MGy), with more homogeneously distributed damage between the four nucleotide types in contrast to the damage preferentially distributed amongst specific protein residues (Fig. 3(b)).

Our findings suggest DNA damage dynamics are indiscriminate of nucleotide identity and are evident only at high doses, where global radiation damage effects are anticipated. Such preferential damage to protein constituents within nucleoprotein complexes in solution has been indicated for the lac repressor-operator (Beguová et al., 2001; Charlier et al., 2002; Eon et al., 2001) and estrogen response element-receptor complexes (Stisova et al., 2006). The accumulated doses typically reported for these aqueous studies (~1 kGy) were much lower than in the C.Esp1396I MX experiment, and conducted at RT where damage is predominantly mediated by $OH^{\bullet}$ radical attack. The C.Esp1396I study additionally provides evidence for preferential protein damage within crystalline nucleoprotein complexes under a high dose regime (MGy) at 100 K, where LEEs act as the dominant damaging species.

Multiple mechanisms have been proposed for DNA radiation-protection by interacting amino acids upon exposure to LEEs, both in solution and the condensed phase through: (a) short-range protein-DNA proton transfer to stabilise LEEs captured by nucleobases, (b) direct electron scavenging by proximal amino acids, and (c) inaccessibility of the nucleotides' lowest unoccupied molecular orbitals (LUMOs) for LEE attachment due to direct engagement with interacting protein (Gu et al., 2014; Solomun and Skalický, 2008). However, for crystalline complexes such as C.Esp1396I, the relevance of such protective mechanisms is unclear, and whether protein is intrinsically more susceptible to X-ray induced damage, or whether the protein scavenges electrons to protect DNA remains to be determined.

3. The TRAP-RNA complex: a model protein-RNA MX damage investigation

An MX SRD experiment has been conducted on the TRAP-RNA complex (Bury et al., 2016), with 10 diffraction datasets ($n=1$, …,10) collected at 100 K on the same crystal over a large dose range (1.31–25.0 MGy). TRAP fortuitously crystallises in a 1:1 ratio of RNA-bound and non-bound protein within the same crystal asymmetric unit (Hopcroft et al., 2002). It thus provides an ideal controlled experiment under identical crystallisation and MX data collection conditions to investigate the exact role of nucleic acid

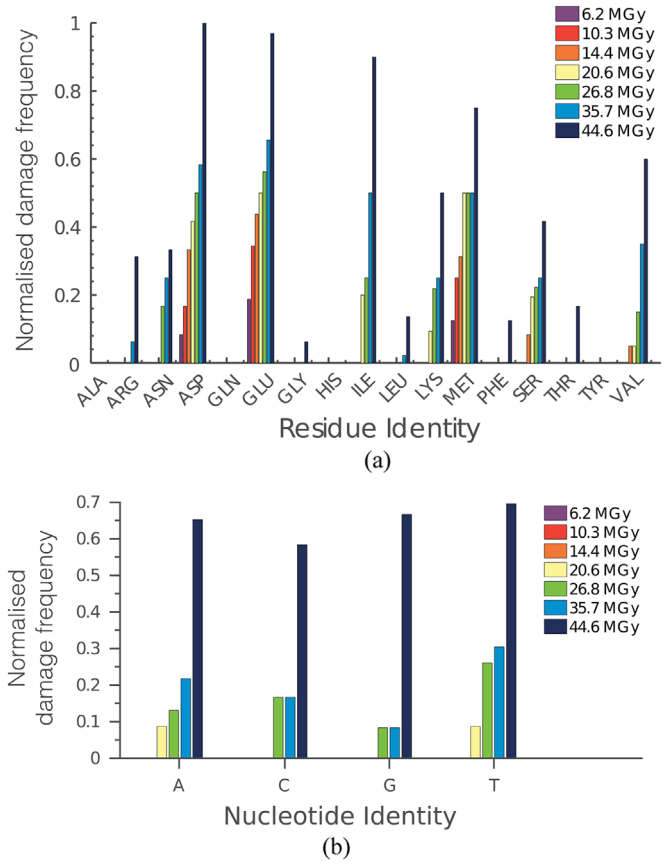

Fig. 3. Normalised frequency of detected SRD events against (a) protein residue type over chains A to D and (b) DNA nucleotides over chains E and F (normalised to the frequency of occurrence of each residue/nucleotide throughout the structure) for each dose (all doses quoted in this review from our work are DWD (Zeldin et al., 2013), diffraction-weighted dose, MGy).

binding on protein damage susceptibility within a crystalline biologically-relevant nucleoprotein complex.

Trp RNA-binding attenuation protein (TRAP) regulates transcription of tryptophan biosynthetic genes in *Bacillus subtilis* and several other bacteria through an attenuation mechanism (Antson et al., 1999). TRAP consists of eleven identical protein chains, arranged as a ring structure with 11-fold rotational symmetry (~91 kDa, Fig. 4(a)). Once activated through binding to L-tryptophan within eleven inter-subunit hydrophobic pockets symmetrically spaced around the TRAP ring, TRAP binds with high-affinity (Elliott et al., 2001) (K_d ~1.1 nM) to a specific RNA sequence within the leader segment of the nascent *trpEDCFBA* operon mRNA. In the current investigation, TRAP is bound to the 53 base RNA sequence $(GAGUU)_{10}GAG$. Bases of G1-A2-G3 nucleotides form direct hydrogen bonds to TRAP, whereas the U4-U5 nucleotides do not bind directly to the protein and are more flexible.

In a procedure similar to that employed in the C.Esp1396I complex investigation, a series of Fourier difference maps ($F_{obs}(n) - F_{obs}(1)$ for datasets n=2, …, 10) were generated to locate SRD sites throughout the large TRAP-RNA complex with increasing dose. A new damage metric, D_{loss}, was introduced as the magnitude of the most negative Fourier difference map value assigned within a local region around each TRAP atom. It was computed for each refined atom at each dose state, in order to quantify, on a per-atom basis, radiation-induced electron density changes within the series of Fourier difference maps (see (Bury et al., 2016) for details). Large positive D_{loss} values indicate radiation-induced atomic disordering reproducibly throughout crystal unit cells, relative to

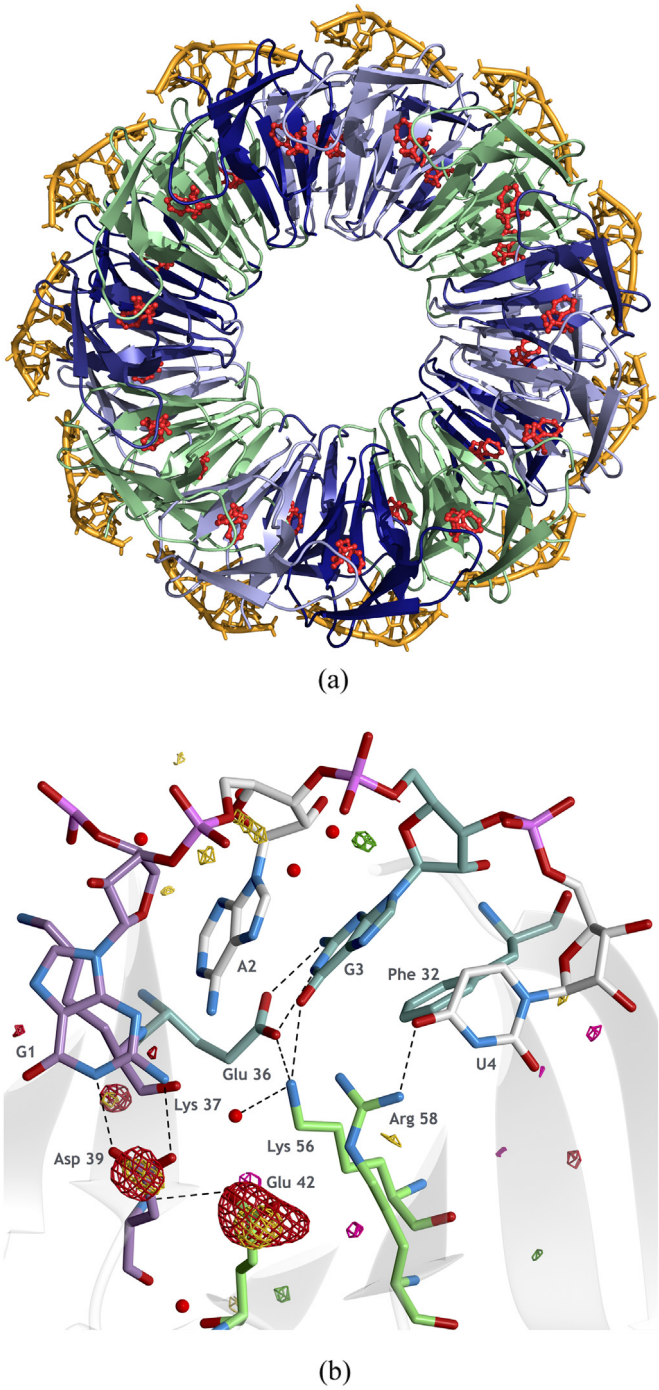

Fig. 4. (a) The TRAP-$(GAGUU)_{10}GAG$ complex asymmetric unit (resolution: 1.98 Å). Bound tryptophan ligands and RNA are represented in red and orange respectively. (b) One of 11 identical RNA-binding interfaces around the RNA-bound TRAP ring (chain N). $F_{obs}(n) - F_{obs}(1)$ Fourier difference maps are overlaid at ±3.5 σ-level, at low-dose (n=2; DWD: 3.88 MGy) in pink/yellow, and high-dose (n=10; DWD: 25.0 MGy) in green/red. (For interpretation of the references to color in this figure legend, the reader is referred to the web version of this article.)

an initial low-dose dataset (here at 1.31 MGy). This approach avoided the previous necessity for visually inspection of Fourier difference maps to detect SRD sites, which has proved a cumbersome limiting factor to previous specific damage investigations in MX (Bury et al., 2015; Fioravanti et al., 2007; Weik et al., 2000).

TRAP is highly Glu and Asp rich (220 in total within the asymmetric unit). However, it does not contain any cysteine or refinable methionine residues. The D_{loss} damage metric

Please cite this article as: Bury, C.S., et al., Radiation damage within nucleoprotein complexes studied by macromolecular X-ray crystallography. Radiat. Phys. Chem. (2016), http://dx.doi.org/10.1016/j.radphyschem.2016.05.023

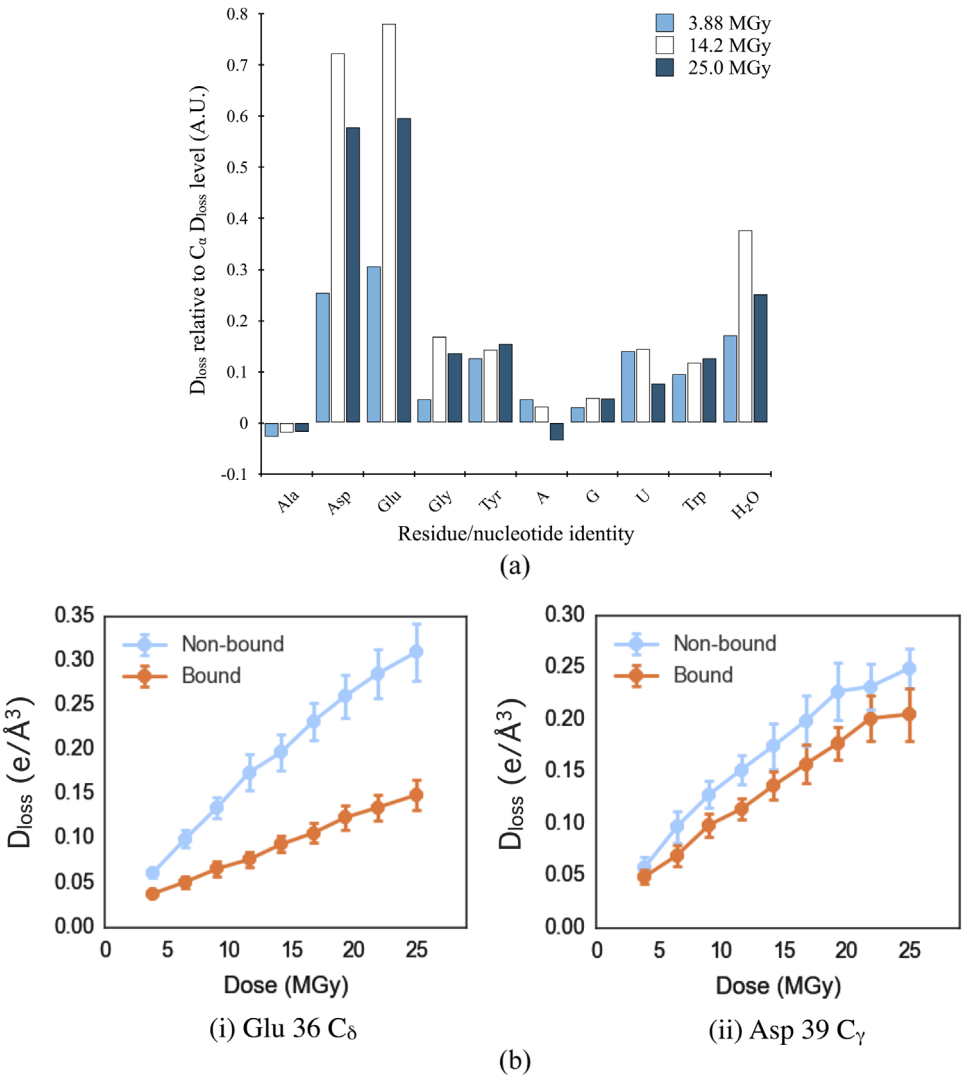

Fig. 5. (a) D_{loss} metric (relative to mean D_{loss} metric over the set of all main-chain protein C_α atoms within TRAP) for a subset of residue and nucleotide types within the asymmetric unit for 3 increasing doses. Positive values indicate greater electron density loss/disordering than that detected for the set of TRAP C_α atoms at the same dose. The TRAP structure only contains non-covalently bound tryptophan ligands, shown at the right of the plot. Damage to ordered solvent is also shown. Note that at the highest doses, global damage increases the non-specific electron density disorder, as evidenced by larger C_α atom D_{loss} values, and this effect decreases the relative D_{loss} of susceptible residue types. (b) D_{loss} progression with increasing dose for (i) Glu-36C_δ and (ii) Asp-39C_γ atoms within TRAP, with atoms grouped by location within the asymmetric unit (RNA-bound or non-bound TRAP ring). 95% confidence intervals are shown, calculated over the 11 equivalent atoms within each ring.

successfully detected typical forms of protein SRD within the TRAP-RNA complex, with Glu and Asp side-chain decarboxylation events interpretable within the first difference map $F_{obs}(2)-F_{obs}(1)$ (Figs. 4(b), 3.9 MGy) and flagged by the D_{loss} metric (Fig. 5(a)). Below 20 MGy, Fourier difference maps revealed negligible radiation-induced electron density deterioration in the region of the refined RNA nucleotides, in direct contrast to the clear protein SRD events noted above. Only above 20 MGy was evidence present for density loss observable around C–O bonds and phosphate groups of the RNA phosphodiester backbone (at dose levels consistent with the C.Esp1396I-DNA study). However, the median D_{loss} calculated over all RNA P atoms at 25 MGy was more than a factor of 2 lower than that of Glu-C_δ and Asp-C_γ atoms, and of the same order as the radiation-insensitive Gly-C_α atoms within TRAP. Therefore little evidence was provided for RNA SSB events consistently throughout the unit cells of the TRAP-RNA crystal, even at high dose values. It was thus concluded that RNA, similarly to DNA, was highly radiation-insensitive relative to protein within crystalline nucleoproteins at 100 K.

For the large number of Glu and Asp residues in TRAP (6 Glu and 4 Asp residues per TRAP monomer) a strong dependence of acidic residue decarboxylation susceptibility on local environment was statistically established using the high 11-fold symmetry around TRAP. The class of acidic residues situated within the 11 identical RNA-binding interfaces distributed around the TRAP ring exhibited greater radiation-induced disordering and subsequent decarboxylation for non-bound TRAP (Fig. 5(b)). The reduction in D_{loss} upon RNA-binding was most significant for Glu-36 (Hotelling T-squared test: p-value$=6.1\times10^{-5}$), the carboxyl side-group of which interacts directly with the G3 nucleobase by accepting two similar length hydrogen bonds ($\sim$2.7 Å on average). In the current TRAP-RNA asymmetric unit, Asp-39 was observed to accept two hydrogen bonds from the two nitrogens of the G1 RNA base, similar to the bonding of Glu-36 to G3. However, a less significant reduction in D_{loss} was observed for Asp-39 upon RNA-binding (Hotelling T-squared test: p-value$=0.093$). We suggest that the relative protection provided by RNA-binding to Glu-36 and Asp-39 directly correlates with the functional importance of each residue in high affinity RNA-binding to TRAP. Whereas nucleoside analogue studies have demonstrated that guanine replacement with

Please cite this article as: Bury, C.S., et al., Radiation damage within nucleoprotein complexes studied by macromolecular X-ray crystallography. Radiat. Phys. Chem. (2016), http://dx.doi.org/10.1016/j.radphyschem.2016.05.023

inosine at position G3 within each repeating GAG triplet resulted in >1000-fold decrease on TRAP binding affinity, inosine substitution at position G1 resulted in less than a 2-fold decrease in binding affinity (Elliott et al., 1999). Indeed, in other crystallographic studies on TRAP (Hopcroft et al., 2004, 2002), Asp-39 is documented to exhibit only a single distorted hydrogen bond to G1, or none at all in the case where G1 is substituted for uracil, without any loss in binding affinity (for TRAP bound to a repeating UAGAU RNA sequence, pdb accession code: 1utf).

The significant reduction in radiation-induced disordering upon RNA-binding was also exhibited for both the aliphatic side-chain of Lys-37 (Hotelling T-squared test, $p=0.024$ for Lys-37C_{ε} atoms) and the aromatic ring of Phe-32 (Hotelling T-squared test, Phe-32C_{ζ}, $p=0.0014$), which stack against bases G1 and G3 within each of the 11 RNA-binding interfaces around TRAP. This finding corresponds well with previous alanine mutagenesis studies, which identified the Lys-37 stacking interaction as essential for high affinity RNA-binding (Yang et al., 1997).

An aqueous RT study on the DNA glycosylase Fpg and its abasic DNA target site (Gillard et al., 2004) has highlighted a similar lower radiation-sensitivity for the protein in its DNA-bound form, through a combination of spectroscopy and mass spectrometry, although at much lower doses (~1 kGy). From this study, it was suggested that the DNA physically shields key protein-DNA interactions sites from hydroxyl mediated-damage, ultimately extending the total *life-dose* of the complex under irradiation. The above findings indicate a short-range protective ability of the RNA to otherwise highly radiation-sensitive protein residues in a crystalline nucleoprotein complex held at 100 K. The stability of the complex is governed by these repeated interactions between the protein and RNA around the TRAP ring. Such complexes may thus also exhibit enhanced life-dose values in a crystalline environment where LEEs are perceived to be the main mediator of radiation-induced structural changes.

4. Conclusion

The striking radiation-insensitivity of crystalline nucleic acids when exposed to X-ray ionising radiation at 100 K during MX data collection is perhaps somewhat surprising given the abundance of observations of LEE-induced covalent bond breakage in RT solution studies on both DNA and RNA, in which much lower doses are accumulated (~1 kGy). It could be postulated that in the crystal environment at 100 K, tight crystal packing could obstruct the development of large nucleic acid deformation events (single strand breakage and base-sugar cleavage) reproducibly throughout crystal unit cells. We also note that much of the radiation chemical investigation of nucleic acids in aqueous solution revolves around OH radical interactions, which we believe to be minimised at the 100 K cryo-temperatures typically used in MX. The dissociative electron attachment (DEA) studies have essentially been conducted on isolated bases in the gas phase (or on solid surfaces under ultrahigh vacuum conditions) where the base is the sole target (Ptasinska and Sanche., 2007). As such, the applicability of these DEA studies is unclear for crystalline nucleic acid polymers interacting with protein at 100 K.

In previous MX radiation damage studies, radiation chemistry literature has been consulted to aid explanation of protein SRD mechanisms within crystals at 100 K. It has been suggested that disulphide bond breakage results from LEE-mediated RSSR group reduction, and that Glu and Asp decarboxylation is induced by oxidative electron-loss centre trapping at their carboxylate group (Burmeister, 2000; Garrison, 1987; Sevilla et al., 1979). However, again the validity in extending such mechanisms to describe the crystalline state at 100 K is questionable, and indeed a more complex, multi-ionisation model for disulphide bridge cleavage (triggered by intersecting LEE tracks) has now been proposed (Sutton et al., 2013). Similarly, for MX experiments conducted on nucleic acids/nucleoprotein crystals held at 100 K, in which accumulated doses approach the order of MGy, it is thus now vital to continue characterising radiation-induced chemistry within the crystalline state, such that damage mechanisms are not falsely extended from studies at quite different regimes (RT, relative low-dose (~kGy), in solution, small oligonucleotides).

The current nucleoprotein MX radiation damage case studies have been presented to motivate further systematic investigations on other complex macromolecules, whilst also describing the introduction of systematic approaches to investigate $F_{obs}(n)-F_{obs}(1)$ Fourier difference maps with minimal subjective bias. In crystals at 100 K, we observe X-ray radiation protection of key RNA-binding residues and localisation of possible DNA phosphate backbone damage at AT-rich sites of high conformational strain. These findings provide an indication of the complexity at which LEE-mediated damage can manifest within intact nucleoprotein complexes. Only with further investigations will the prevalence of such damage events within the diverse community of nucleoprotein complexes be determined and the underlying mechanisms governing such damage dynamics elucidated.

Acknowledgements

We gratefully acknowledge the UK Engineering and Physical Sciences Research Council (Grant: EP/G03706X/1) for studentship funding in the Systems Biology Programme of the University of Oxford Doctoral Training Centre (CSB). IC is supported by the US Department of Energy Office of Science, Office of Basic Energy Sciences under Award Number DE-FC02–04ER1553.

References

Alizadeh, E., Orlando, T.M., Sanche, L., 2015. Biomolecular damage induced by ionizing radiation: the direct and indirect effects of low-energy electrons on DNA. Annu. Rev. Phys. Chem. 66, 379–398.

Alizadeh, E., Sanche, L., 2014. Low-energy-electron interactions with DNA: approaching cellular conditions with atmospheric experiments. Eur. Phys. J. D 68, 1–13.

Alizadeh, E., Sanz, A.G., García, G., Sanche, L., 2013. Radiation damage to DNA: the indirect effect of low energy electrons. J. Phys. Chem. Lett. 19, 820–825.

Allan, E.G., Kander, M.C., Carmichael, I., Garman, E.F., 2013. To scavenge or not to scavenge, that is STILL the question. J. Synchrotron Radiat. 20, 23–36.

Antson, A.A., Dodson, E.J., Dodson, G., Greaves, R.B., Chen, X., Gollnick, P., 1999. Structure of the trp RNA-binding attenuation protein, TRAP, bound to RNA. Nature 401, 235–242.

Ball, N., Streeter, S.D., Kneale, G.G., McGeehan, J.E., 2009. Structure of the restriction-modification controller protein C.Esp1396I. Acta Cryst. D Biol. Cryst. 65, 900–905.

Barrios, R., Skurski, P., Simons, J., 2002. Mechanism for damage to DNA by low-energy electrons. J. Phys. Chem. B 106, 7991–7994.

Begusová, M., Eon, S., Sy, D., Culard, F., Charlier, M., Spotheim-Maurizot, M., 2001. Radiosensitivity of DNA in a specific protein-DNA complex: the lac repressor-lac operator complex. Int. J. Radiat. Biol. 77, 645–654.

Berdys, J., Skurski, P., Simons, J., 2004. Damage to model DNA fragments by 0.25–1.0 eV electrons attached to a thymine pi* orbital. J. Phys. Chem. B 108, 5800–5805.

Borshchevskiy, V., Round, E., Erofeev, I., Weik, M., Ishchenko, A., Gushchin, I., Mishin, A., Willbold, D., Buldt, G., Gordeliy, V., 2014. Low-dose X-ray radiation induces structural alterations in proteins. Acta Cryst. D Biol. Cryst. 70, 2675–2685.

Boudaïffa, B., 2000. Resonant formation of DNA strand breaks by low-energy (3–20 eV) electrons. Science 287, 1658–1660.

Burmeister, W.P., 2000. Structural changes in a cryo-cooled protein crystal owing to radiation damage. Acta Cryst. D Biol. Cryst. 56, 328–341.

Bury, C., Garman, E.F., Ginn, H.M., Ravelli, R.B., Carmichael, I., Kneale, G., McGeehan, J.E., 2015. Radiation damage to nucleoprotein complexes in macromolecular crystallography. J. Synchrotron Radiat. 22, 213–224.

Bury, C.S., McGeehan, J.E., Antson, A.A., Carmichael, I., Gerstel, M., Shevtsov, M.B., Garman, E.F., 2016. RNA protects a nucleoprotein complex against radiation

damage. Acta Cryst. D. Biol. Cryst. 75, 648–657.
Cadet, J., Delatour, T., Douki, T., Gasparutto, D., Pouget, J.P., Ravanat, J.L., Sauvaigo, S., 1999. Hydroxyl radicals and DNA base damage. Mutat. Res. 424, 9–21.
Chance, M.R., Sclavi, B., Woodson, S.A., Brenowitz, M., 1997. Examining the conformational dynamics of macromolecules with time-resolved synchrotron X-ray 'footprinting'. Structure 5, 865–869.
Charlier, M., Eon, S., Sèche, E., Bouffard, S., Culard, F., Spotheim-Maurizot, M., 2002. Radiolysis of lac repressor by gamma-rays and heavy ions: a two-hit model for protein inactivation. Biophys. J. 82, 2373–2382.
Czapla-Masztafiak, J., Szlachetko, J., Milne Christopher, J., Lipiec, E., Sá, J., Penfold Thomas, J., Huthwelker, T., Borca, C., Abela, R., Kwiatek Wojciech, M., 2016. Investigating DNA radiation damage using X-ray absorption spectroscopy. Biophys. J. 110, 1304–1311.
De La Mora, E., Carmichael, I., Garman, E.F., 2011. Effective scavenging at cryotemperatures: further increasing the dose tolerance of protein crystals. J. Synchrotron Radiat. 18, 346–357.
Elliott, M.B., Gottlieb, Pa, Gollnick, P., 1999. Probing the TRAP-RNA interaction with nucleoside analogs. RNA 5, 1277–1289.
Elliott, M.B., Gottlieb, P.A., Gollnick, P., 2001. The mechanism of RNA binding to TRAP: initiation and cooperative interactions. RNA 7, 85–93.
Eon, S., Culard, F., Sy, D., Charlier, M., Spotheim-Maurizot, M., 2001. Radiation disrupts protein–DNA complexes through damage to the protein. The lac repressor–operator system. Radiat. Res. 156, 110–117.
Ferreira, K.N., Iverson, T.M., Maghlaoui, K., Barber, J., Iwata, S., 2004. Architecture of the photosynthetic oxygen-evolving center. Science 303, 1831–1838.
Fioravanti, E., Vellieux, F.M., Amara, P., Madern, D., Weik, M., 2007. Specific radiation damage to acidic residues and its relation to their chemical and structural environment. J. Synchrotron Radiat. 14, 84–91.
Garman, E.F., 2010. Radiation damage in macromolecular crystallography: what is it and why should we care? Acta Cryst. D Biol. Cryst. 66, 339–351.
Garrison, W.M., 1987. Reaction mechanisms in the radiolysis of peptides, polypeptides, and proteins. Chem. Rev. 87, 381–398.
Gerstel, M., Deane, C.M., Garman, E.F., 2015. Identifying and quantifying radiation damage at the atomic level. J. Synchrotron Radiat. 22, 201–212.
Gillard, N., Begusova, M., Castaing, B., Spotheim-Maurizot, M., 2004. Radiation affects binding of Fpg repair protein to an abasic site containing DNA. Radiat. Res. 162, 566–571.
Gu, B., Smyth, M., Kohanoff, J., 2014. Protection of DNA against low-energy electrons by amino acids: a first-principles molecular dynamics study. PCCP 16, 24350–24538.
Holton, J.M., 2009. A beginner's guide to radiation damage. J. Synchrotron Radiat. 16, 133–142.
Hopcroft, N.H., Manfredo, A., Wendt, A.L., Brzozowski, A.M., Gollnick, P., Antson Aa, 2004. The interaction of RNA with TRAP: the role of triplet repeats and separating spacer nucleotides. J. Mol. Biol. 338, 43–53.
Hopcroft, N.H., Wendt, A.L., Gollnick, P., Antson, A.A., 2002. Specificity of TRAP-RNA interactions: crystal structures of two complexes with different RNA sequences. Acta Cryst. D Biol. Cryst. 58, 615–621.
Jones, G.D., Lea, J.S., Symons, M.C., Taiwo, F.A., 1987. Structure and mobility of electron gain and loss centres in proteins. Nature 330, 772–773.
McGeehan, J.E., Carpentier, P., Royant, A., Bourgeois, D., Ravelli, R.B.G., 2007. X-ray radiation-induced damage in DNA monitored by online Raman. J. Synchrotron Radiat. 14, 99–108.
McGeehan, J.E., Streeter, S.D., Thresh, S.J., Ball, N., Ravelli, R.B., Kneale, G.G., 2008. Structural analysis of the genetic switch that regulates the expression of restriction-modification genes. Nucleic Acids Res. 36, 4778–4787.
Michaud, M., Bazin, M., Sanche, L., 2012. Measurement of inelastic cross sections for low-energy electron scattering from DNA bases. Int. J. Radiat. Biol. 88, 15–21.
Murray, J., Garman, E., 2002. Investigation of possible free-radical scavengers and metrics for radiation damage in protein cryocrystallography. J. Synchrotron Radiat. 9, 347–354.
Nave, C., Hill, M.A., 2005. Will reduced radiation damage occur with very small crystals? J. Synchrotron Radiat. 12, 299–303.
O'Neill, P., Stevens, D.L., Garman, E.F., 2002. Physical and chemical considerations of damage induced in protein crystals by synchrotron radiation: a radiation chemical perspective. J. Synchrotron Radiat. 9, 329–332.
Owen, R.L., Axford, D., Nettleship, J.E., Owens, R.J., Robinson, J.I., Morgan, A.W., Dore, A.S., Lebon, G., Tate, C.G., Fry, E.E., Ren, J., Stuart, D.I., Evans, G., 2012. Outrunning free radicals in room-temperature macromolecular crystallography. Acta Cryst. D Biol. Cryst. 68, 810–818.
Owen, R.L., Paterson, N., Axford, D., Aishima, J., Schulze-Briese, C., Ren, J., Fry, E.E., Stuart, D.I., Evans, G., 2014. Exploiting fast detectors to enter a new dimension in room-temperature crystallography. Acta Cryst. D Biol. Cryst. 70, 1248–1256.
Owen, R.L., Rudino-Pinera, E., Garman, E.F., 2006. Experimental determination of the radiation dose limit for cryocooled protein crystals. Proc. Natl. Acad. Sci. USA 103, 4912–4917.
Ptasinska, S., Sanche, L., 2007. Dissociative electron attachment to hydrated single DNA strands. Phys. Rev. E 75, 031915.
Ravelli, R.B.G., Garman, E.F., 2006. Radiation damage in macromolecular cryocrystallography. Curr. Opin. Struct. Biol. 16, 624–629.
Sanishvili, R., Yoder, D.W., Pothineni, S.B., Rosenbaum, G., Xu, S., Vogt, S., Stepanov, S., Makarov, Oa, Corcoran, S., Benn, R., NagarajanV, R., Smith, J.L., Fischetti, R.F., 2011. Radiation damage in protein crystals is reduced with a micron-sized X-ray beam. Proc. Natl. Acad. Sci. USA 108, 6127–6132.
Sevilla, M.D., D'Arcy, J.B., Morehouse, K.M., 1979. An electron spin resonance study of γ-irradiated frozen aqueous solutions containing dipeptides. Mechanisms of radical reaction. J. Phys. Chem. 83, 2887–2892.
Simons, J., 2006. How do low-energy (0.1–2 eV) electrons cause DNA-strand breaks? Acc. Chem. Res. 39, 772–779.
Solomun, T., Skalický, T., 2008. The interaction of a protein–DNA surface complex with low-energy electrons. Chem. Phys. Lett. 453, 101–104.
Southworth-Davies, R.J., Medina, M.A., Carmichael, I., Garman, E.F., 2007. Observation of decreased radiation damage at higher dose rates in room temperature protein crystallography. Structure 15, 1531–1541.
Spotheim-Maurizot, M., Davidkova, M., 2011. Radiation damage to DNA in DNA-protein complexes. Mutat. Res. 711, 41–48.
Stellato, F., Oberthur, D., Liang, M., Bean, R., Gati, C., Yefanov, O., Barty, A., Burkhardt, A., Fischer, P., Galli, L., Kirian, R.A., Meyer, J., Panneerselvam, S., Yoon, C.H., Chervinskii, F., Speller, E., White, T.A., Betzel, C., Meents, A., Chapman, H.N., 2014. Room-temperature macromolecular serial crystallography using synchrotron radiation. IUCrJ 1, 204–212.
Stisova, V., Goffinont, S., Spotheim-Maurizot, M., Davidkova, M., 2006. Radiation damage to DNA-protein specific complexes: estrogen response element-estrogen receptor complex. Radiat. Prot. Dosim. 122, 106–109.
Sutton, K.A., Black, P.J., Mercer, K.R., Garman, E.F., Owen, R.L., Snell, E.H., Bernhard, W.A., 2013. Insights into the mechanism of X-ray-induced disulfide-bond cleavage in lysozyme crystals based on EPR, optical absorption and X-ray diffraction studies. Acta Cryst. D Biol. Cryst. 69, 2381–2394.
Symons, M.C.R., 1997. Electron movement through proteins and DNA. Free Radic. Biol. Med. 22, 1271–1276.
Théodore, M., Sobczyk, M., Simons, J., 2006. Cleavage of thymine N3–H bonds by low-energy electrons attached to base π^* orbitals. Chem. Phys. 329, 139–147.
Voorhees, R.M., Weixlbaumer, A., Loakes, D., Kelley, A.C., Ramakrishnan, V., 2009. Insights into substrate stabilization from snapshots of the peptidyl transferase center of the intact 70S ribosome. Nat. Struct. Mol. Biol. 16, 528–533.
Weik, M., Ravelli, R.B., Kryger, G., McSweeney, S., Raves, M.L., Harel, M., Gros, P., Silman, I., Kroon, J., Sussman, J.L., 2000. Specific chemical and structural damage to proteins produced by synchrotron radiation. Proc. Natl. Acad. Sci. USA 97, 623–628.
Yang, M., Chen, Xp, Militello, K., Hoffman, R., Fernandez, B., Baumann, C., Gollnick, P., 1997. Alanine-scanning mutagenesis of *Bacillus Subtilis* trp RNA-binding attenuation protein (TRAP) reveals residues involved in tryptophan binding and RNA binding. J. Mol. Biol. 270, 696–710.
Yano, J., Kern, J., Irrgang, K.D., Latimer, M.J., Bergmann, U., Glatzel, P., Pushkar, Y., Biesiadka, J., Loll, B., Sauer, K., Messinger, J., Zouni, A., Yachandra, V.K., 2005. X-ray damage to the Mn4Ca complex in single crystals of photosystem II: a case study for metalloprotein crystallography. Proc. Natl. Acad. Sci. USA 102, 12047–12052.
Zeldin, O.B., Brockhauser, S., Bremridge, J., Holton, J.M., Garman, E.F., 2013. Predicting the X-ray lifetime of protein crystals. Proc. Natl. Acad. Sci. USA 110, 20551–20556.

Please cite this article as: Bury, C.S., et al., Radiation damage within nucleoprotein complexes studied by macromolecular X-ray crystallography. Radiat. Phys. Chem. (2016), http://dx.doi.org/10.1016/j.radphyschem.2016.05.023